



## Conference Paper

# **Solid formation in ammonia-based processes for CO<sub>2</sub> capture- Turning a challenge into an opportunity**

**Author(s):**

Sutter, Daniel; Gazzani, Matteo; Pérez-Calvo, José-Francisco; Leopold, Clemens; Milella, Federico; Mazzotti, Marco

**Publication Date:**

2017-07

**Permanent Link:**

<https://doi.org/10.3929/ethz-b-000233984> →

**Originally published in:**

Energy Procedia 114, <http://doi.org/10.1016/j.egypro.2017.03.1229> →

**Rights / License:**

[Creative Commons Attribution-NonCommercial-NoDerivatives 4.0 International](#) →

This page was generated automatically upon download from the [ETH Zurich Research Collection](#). For more information please consult the [Terms of use](#).



13th International Conference on Greenhouse Gas Control Technologies, GHGT-13, 14-18  
November 2016, Lausanne, Switzerland

## Solid formation in ammonia-based processes for CO<sub>2</sub> capture – Turning a challenge into an opportunity

Daniel Sutter, Matteo Gazzani, José-Francisco Pérez-Calvo, Clemens Leopold, Federico Milella, Marco Mazzotti\*  
*Institute of Process Engineering, ETH Zurich, Sonneggstrasse 3, 8092 Zurich, Switzerland*

### Abstract

This article gives an overview of our holistic approach for the optimization of the Chilled Ammonia Process by (i) understanding the thermodynamics and kinetics of solid formation in the CO<sub>2</sub>-NH<sub>3</sub>-H<sub>2</sub>O system and finding criticalities with respect to solid formation in the process, and by (ii) exploiting solid formation to reduce the energy penalty of CO<sub>2</sub> capture by developing a new process, the Controlled Solid Formation-Chilled Ammonia Process. Recent advances in the construction of phase diagrams as well as in the optimization of the new process are highlighted.

© 2017 Published by Elsevier Ltd. This is an open access article under the CC BY-NC-ND license

(<http://creativecommons.org/licenses/by-nc-nd/4.0/>).

Peer-review under responsibility of the organizing committee of GHGT-13.

**Keywords:** Chilled ammonia, CO<sub>2</sub>-NH<sub>3</sub>-H<sub>2</sub>O system, ternary phase diagrams, process optimization, thermodynamics, kinetics

### Nomenclature

ATR-FTIR	Attenuated Total Reflectance-Fourier Transform Infrared spectroscopy
BC	Ammonium bicarbonate, NH <sub>4</sub> HCO <sub>3</sub>
CAP	Chilled Ammonia Process
CB	Ammonium carbonate hydrate, (NH <sub>4</sub> ) <sub>2</sub> CO <sub>3</sub> · H <sub>2</sub> O
CM	Ammonium carbamate, NH <sub>2</sub> COONH <sub>4</sub>

\* Corresponding author. Tel.: +41 44 632 2456; fax: +41 44 632 1141.

E-mail address: [marco.mazzotti@ipe.mavt.ethz.ch](mailto:marco.mazzotti@ipe.mavt.ethz.ch)

CSF-CAP	Controlled solid formation-chilled ammonia process
L	Liquid
S	Solid
SC	Ammonium sesqui-carbonate, $(\text{NH}_4)_2\text{CO}_3 \cdot 2\text{NH}_4\text{HCO}_3$
SLE	Solid-liquid equilibrium
SPECCA	Specific primary energy per $\text{CO}_2$ avoided
V	Vapor
VLE	Vapor-liquid equilibrium

## 1. Introduction

The Chilled Ammonia Process (CAP) is a promising technology for post-combustion  $\text{CO}_2$  capture that shows a competitive energetic performance compared to conventional amines. The use of aqueous  $\text{NH}_3$  as a solvent offers advantages concerning global availability, environmental footprint, and cost. Contrary to amines, where solvent degradation calls for reclaiming units and a constant make-up of the relatively expensive amines, the  $\text{NH}_3$  solvent is chemically stable in the presence of oxygen and of impurities, such as  $\text{SO}_x$  and  $\text{NO}_x$ .

Possible clogging of process equipment due to solid formation is a known disadvantage of  $\text{NH}_3$ -based  $\text{CO}_2$  capture processes. Accordingly, the current CAP implementations avoid solid formation in the absorber by limiting the  $\text{NH}_3$  and  $\text{CO}_2$  concentration [1,2]. On the other hand, a high  $\text{CO}_2$  uptake capacity is an important parameter to limit the energy penalty of the regeneration. Therefore, we have developed a new process that turns the challenge of solid formation into an opportunity by controlling the precipitation and by exploiting the potential of a phase-change in the solvent [3].

The new Controlled Solid Formation-Chilled Ammonia Process (CSF-CAP) controls the formation, separation, and subsequent dissolution of solids in a dedicated process section, whereas the absorption and stripping columns are kept free of solids. Our holistic process development strategy comprises (i) thermodynamics and (ii) kinetics, (iii) process synthesis, (iv) process integration, and (v) process optimization. This work summarizes the development considering all 5 aspects and highlights important recent additions.

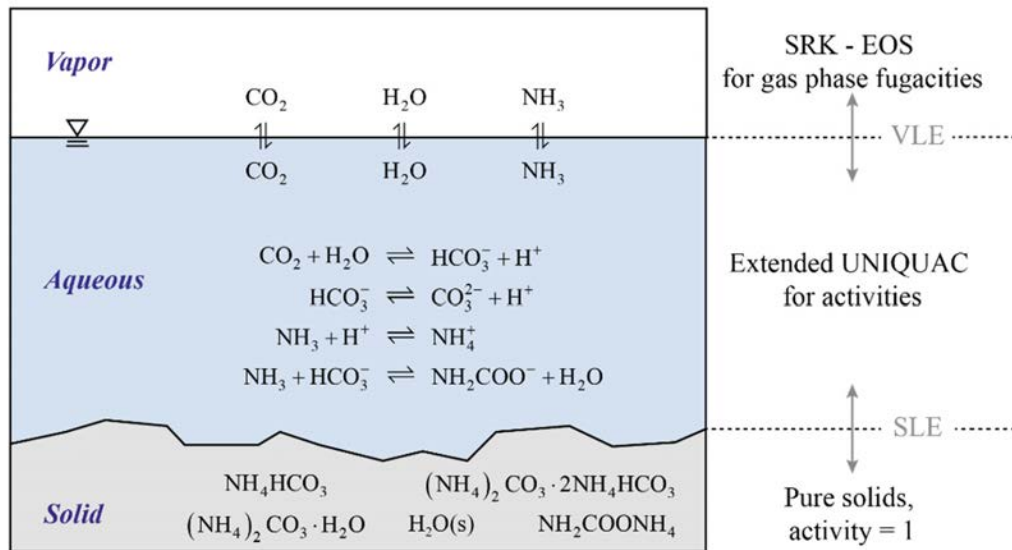


Fig. 1: The  $\text{CO}_2$ - $\text{NH}_3$ - $\text{H}_2\text{O}$  system as described by the Thomsen model [7].

## 2. Thermodynamics and phase diagram construction

The  $\text{CO}_2\text{-NH}_3\text{-H}_2\text{O}$  system is characterized by the complex interaction between a weak base and a weak acid in the aqueous phase. Including the self-ionization of water and ice formation, there are in total 5 coupled reaction equilibria, 5 solid-liquid equilibria (SLE), and 3 vapor-liquid equilibria (VLE) to be considered. Our work relies on the thermodynamic model developed by Thomsen and Rasmussen [4] and Darde et al. [5], in the following called “Thomsen model”. Fig. 1 illustrates the thermodynamic system and the model.

Ternary phase diagrams of the  $\text{CO}_2\text{-NH}_3\text{-H}_2\text{O}$  system proved to be a powerful tool in the analysis and optimization of the CAP [3,6]. These diagrams are based on the thermodynamic model described above. Their construction involves a two-step screening algorithm that relies only on flash calculations and can be applied to any thermodynamic model without requiring changes to the source code of the model. In **step 1**, the phase diagram is constructed with the 3 pure components in the corners and the intermediate solid compounds located according to their pure composition in weight fractions (see Fig. 2a). A grid is created by defining 100 points on the  $\text{H}_2\text{O-NH}_3$  binary, i.e. the right-hand-side edge of the ternary phase diagram and by connecting them to the  $\text{CO}_2$ -vertex (see gray lines in Fig. 2a). 1000 steps are defined along each of these 100 lines, resulting in a “radial” grid around the  $\text{CO}_2$ -vertex with  $10^5$  grid points. This special grid geometry was chosen to resemble the conditions in the absorber and desorber of the CAP. Physically, the gray lines represent an aqueous ammonia solution that is gradually loaded with  $\text{CO}_2$ . An algorithm has been developed in Matlab that calls the Thomsen model in Aspen Plus and runs a flash calculation at a given temperature and pressure for each grid point. The algorithm detects any appearance or disappearance of a solid (S), liquid (L), or vapor (V) phase in the resulting equilibrium composition with respect to the surrounding points of the grid and plots the phase boundary at the grid point where the appearance or disappearance occurred. Thus, the resulting phase diagram has an accuracy of 0.001 (in weight fraction) in the  $\text{CO}_2$  direction and 0.01 in the  $\text{NH}_3$ -direction. Grid points where the thermodynamic model did not converge are marked.

In **step 2**, the phase diagram generated as described above is analyzed and a new simplified grid is developed. Fig. 2b shows the phase diagram at 1 bar and  $25^\circ\text{C}$  as an example. The new grid exploits the Gibbs phase rule and requires only 2 grid lines in this example (shown in gray). According to the Gibbs phase rule, 3-phase regions in a 3-component system have zero degrees of freedom at isobaric and isothermal conditions, meaning that the composition of each phase is fixed. Hence, a 3-phase region has a triangular shape with straight boundaries, in which the vertexes of the triangle represent the three phase compositions. A single flash calculation for one grid point in the 3-phase region is sufficient to plot the entire region, by simply connecting the three phase compositions with straight lines. Every equilibrium composition within the 3-phase triangle consists of these three phases with their fixed composition, only the weight fraction of one phase over the other phases may change. The lever-arm rule can be applied to find the weight fraction of each phase graphically.

Similarly, a 2-phase region has one degree of freedom, meaning that the composition of the two phases can vary, but they are directly correlated. For an L+V 2-phase region, there is only one equilibrium composition of phase V for every given composition of phase L. In a graphical representation, this means that the two phase compositions in equilibrium are connected by a straight tieline. Based on these considerations, a 2-phase region consists of two curved lines for the variable phase compositions, and two straight lines which represent the outermost tielines. If one of the two phases is a pure solid, one of the curved lines collapses into a single point, which corresponds to the composition of the solid. In order to determine the phase boundaries of a 2-phase region, flash calculations along a grid line that scans the region from one extreme tieline to the other are required. Each of the flashes along the grid line yields two phase compositions that are in equilibrium, e.g. the composition of the L-phase and of the V-phase. By connecting all the L-phase compositions and all the V-phase compositions, we can plot the two curved boundaries of the 2-phase region. By adding the two extreme tielines on either side, the region can be completed. Again, if one of the phases is a pure solid, one of the curved lines collapses into a single point, but the construction follows the same principles.

Based on the above considerations, a sufficient grid for the phase diagram calculations needs at least one point in each 3-phase region and should scan the 2-phase regions ideally orthogonally to their tielines. Thus, the phase diagrams generated in the first step are analyzed and a simplified grid is developed. For the conditions prevailing in the absorption section of the CAP, i.e. around 1 bar and  $0\text{--}45^\circ\text{C}$ , the two lines shown in Fig. 2b are sufficient.

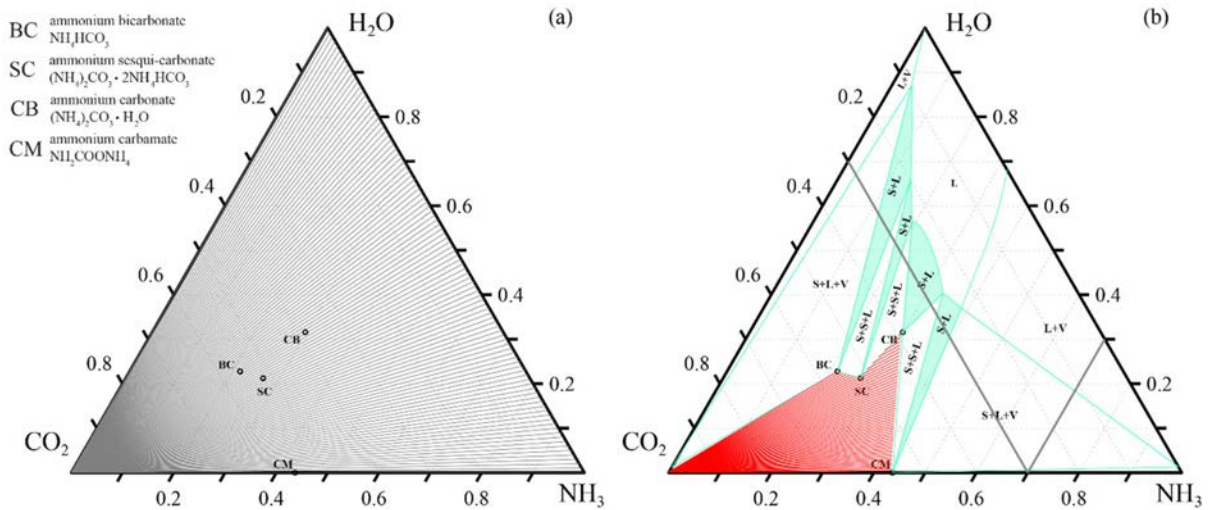


Fig. 2: Construction of ternary phase diagrams for the  $\text{CO}_2$ - $\text{NH}_3$ - $\text{H}_2\text{O}$  system. (a) Ternary diagram in weight fractions indicating the exact composition of the pure intermediate solid compounds and showing the geometry of the grid used in the screening for phase boundaries. (b) Phase diagram at 25°C and 1 bar in weight fractions. The two gridlines for the second step in the phase diagram construction are shown in gray. The region shaded in red indicates the grid points where the thermodynamic model did not converge or produced non-physical output. Please note that for both L+V regions in this example the curved line representing the V-phase compositions are too small to be visible, despite actually being present, as can be revealed with a zoom-in in the original vector graphic.

The two steps combined present a robust and precise tool to generate ternary phase diagrams. The first algorithm with  $10^5$  grid points is used to screen the entire diagram and to get a general understanding of the phase regions present for a given range of temperature and pressure. Then, the reduced grid for step 2 is defined and the second algorithm is used to increase the precision while reducing the computational cost. For example, it allows the rapid generation of phase diagrams for a set of conditions of particular interest in the process. Fewer flash calculations are required (typically  $10^3$  grid points per line are sufficient) and smaller amounts of data are needed to find the phase boundaries. While the precision of the first algorithm is defined by the resolution of the grid, step 2 utilizes the exact phase composition to plot the phase boundaries. Thus, the precision is defined by the thermodynamic model itself.

### 3. Equilibrium-based process modeling

Our work on process modeling includes a comprehensive analysis of the conventional CAP with a focus on criticalities with respect to solid formation and opportunities for optimization [7]. This analysis relies extensively on the use of phase diagrams of the  $\text{CO}_2$ - $\text{NH}_3$ - $\text{H}_2\text{O}$  system. The phase diagrams have been validated using phase diagrams for the binary systems  $\text{H}_2\text{O}$ - $\text{NH}_3$ ,  $\text{H}_2\text{O}$ - $\text{CO}_2$ , and  $\text{CO}_2$ - $\text{NH}_3$  from the literature and their application is described in detail [7]. The composition of the various process streams is mapped on the phase diagrams, which proved to be a powerful visual tool in analyzing the process units under different operating conditions. As a major result, a trade-off between maximizing the  $\text{CO}_2$ -concentration in the rich stream and preventing solid formation in the pumparound was identified. The analysis clearly revealed that the energetic optimization pushes the solvent composition towards the solubility limit.

In the new CSF-CAP, the rich solution is cooled in a crystallization unit to induce precipitation (see Fig. 3). Ammonium bicarbonate (BC) forms at low temperature and the generated suspension is separated in a hydrocyclone into (i) a rich slurry, which is sent to regeneration, and (ii) a clear solution, which is recycled to the absorber. The recycle serves as a highly efficient pumparound: Due to the solid formation and separation, the recycle can be introduced at lower temperature and enables a more effective control of the  $\text{NH}_3$ -slip. In this way, the solid formation allows decoupling the low temperature needed for the pumparound and the high  $\text{CO}_2$  solvent concentration desired for the regeneration; the above-described trade-off is resolved. Again, the phase diagram

representation has been used extensively to analyze and optimize the new process. In fact, the use of phase diagrams to compare the conventional CAP and the CSF-CAP and the mapping of additional thermodynamic properties on the diagrams (such as the equilibrium partial pressure of  $\text{CO}_2$  and  $\text{NH}_3$ ) in Sutter et al. [3] led to the introduction of the above-described second step in the phase diagram construction.

#### 4. Kinetics

Our investigation of the kinetics includes both mass transfer and solid formation. The development of a rate-based model for the absorption is described in another work submitted to GHGT-13 [8]. Furthermore, nucleation and growth rates of ammonium bicarbonate were determined experimentally. Such measurements are complicated by the high volatility of  $\text{CO}_2$  and  $\text{NH}_3$ , which prohibits the application of many state-of-the-art experimental techniques in the field of crystallization. The developed experimental setup is based on a temperature-controlled reactor operating in batch mode. The volume of the vapor phase in the reactor is kept small enough to allow neglecting the influence of the VLE on the liquid composition. Based on this approach,  $\text{CO}_2$ - $\text{NH}_3$ - $\text{H}_2\text{O}$ -solutions with known composition can be generated by dissolving ammonium bicarbonate in water and optionally in concentrated ammonium solution. The nucleation rate parameters were identified using the polythermal method [9], which yields valuable metastable zone width data in parallel. Growth rates can be inferred from the concentration profile during a cooling crystallization experiment with the help of a population balance model. The in-situ concentration measurements were based on Attenuated Total Reflectance-Fourier Transform Infrared (ATR-FTIR) spectroscopy. A calibration of the ATR-FTIR for the  $\text{CO}_2$ - $\text{NH}_3$ - $\text{H}_2\text{O}$  system has been developed, applying multivariate calibration techniques to enable precise concentration measurements despite the complex IR-spectrum with overlapping peaks of the individual species. The results of the calibration campaign and the growth kinetics will be published shortly.

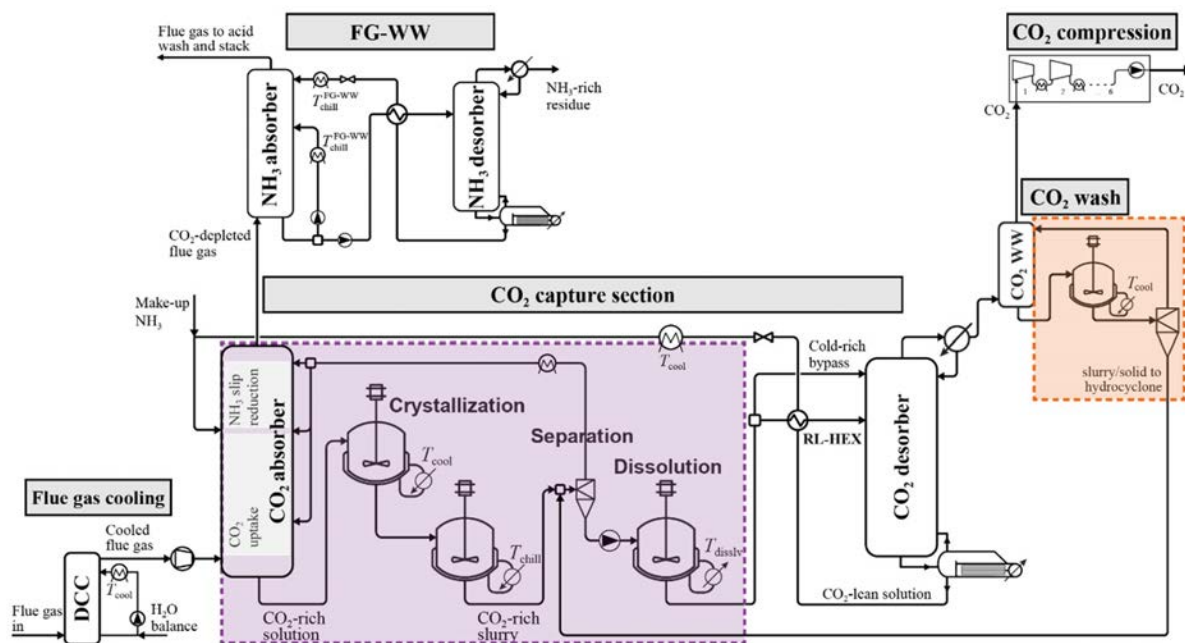


Fig. 3: Flowscheme of the CSF-CAP. The colored squares highlight the sections that differ compared to the conventional CAP without solid formation. Adapted from [3].

## 5. Process synthesis and process integration

In the synthesis of the CSF-CAP, several variations of the solid handling section have been compared with respect to their practicality on an industrial scale, heat integration opportunities, and energetic performance. The resulting scheme considers a two-step cooling that exploits the available cooling water and the integration of crystallization and dissolution in scraped-surface crystallizers, a double-walled tubular reactor that enables heat exchange between the dissolving and the crystallizing suspension [3].

## 6. Process optimization

The optimization of absorption-based CO<sub>2</sub> capture processes is challenging because of (i) the different nature of the energy requirements of the process, i.e. thermal energy for heating and cooling vs. electric energy, (ii) the vast design space with a large number of degrees of freedom, especially when changes in the flowscheme are included, and (iii) the complex thermodynamics with multiple VLE, SLE, and speciation equilibria hampering the numerical convergence of the process simulations.

Our optimization strategy relies on a rigorous performance assessment based on the Specific Primary Energy Consumption for CO<sub>2</sub> Avoided (SPECCA) as the objective function. The SPECCA is computed by integrating the CAP with a reference power plant [10]. Furthermore, an automated algorithm relying on a Matlab routine which controls and evaluates process simulations in Aspen Plus was developed, in order to be able to run a large number of simulations with multiple input parameter combinations.

The CSF-CAP increases the CO<sub>2</sub>-concentration of the stream that enters the regeneration section significantly by forming ammonium bicarbonate solids and by increasing the slurry density in a subsequent partial solid-liquid separation. Therefore, the specific heat demand per unit mass of CO<sub>2</sub> of the regeneration can be reduced by up to 30% compared to the conventional CAP. On the contrary, the crystallization requires additional cooling and the electricity demand for refrigeration increases. As a consequence, the performance of the CSF-CAP strongly depends on the assumptions that affect the energy cost of cooling and heating and on the level of heat integration that can be achieved. In the analysis presented in Sutter et al. [3], a fixed level of heat integration and a fixed coefficient of performance (COP) were assumed in the optimization algorithm. A post-ex pinch analysis showed, that the level of heat integration assumed was difficult to achieve with the optimal operating conditions. Therefore, we have implemented the pinch analysis within the optimization routine in the meantime. It determines the correct level of heat integration for each set of operating conditions individually and a fixed assumption is no longer required. After scanning a subset of the variable space, we have achieved a SPECCA of 2.62 MJ/kg<sub>CO<sub>2</sub></sub>, with a COP of 6.5 and a cooling water temperature of 15°C, which confirms the results given in Sutter et al. [3] and the significant improvement compared to the conventional CAP with an optimal SPECCA of 2.93 MJ/kg<sub>CO<sub>2</sub></sub>.

## 7. Conclusions

The optimization of complex processes, such as post-combustion CO<sub>2</sub> capture processes, requires a systematic understanding of the relevant thermodynamics and kinetics in combination with rigorous process synthesis and process integration. Phase diagrams are a valuable visual tool that can support various parts of such a holistic optimization approach, especially when the system thermodynamics are complex, as in the case of the CAP.

A method for the construction of precise ternary phase diagrams with general applicability to any thermodynamic system/model has been presented. Our activities concerning the investigation of the thermodynamics and kinetics of the CO<sub>2</sub>-NH<sub>3</sub>-H<sub>2</sub>O system and the process synthesis and process integration have been summarized. An extension of the optimization algorithm presented earlier [3] and first results of its application are given.

## Acknowledgement

We acknowledge funding within CTI-project 13973.1 by the Swiss Commission for Technology and Innovation (CTI) in cooperation with Alstom Switzerland Ltd. Additionally, the authors would like to thank Kaj Thomsen (Department of Chemical and Biochemical Engineering, Technical University of Denmark) for making the thermodynamics model available, for providing the relevant software, and for giving precious advice.

## References

- [1] H. Yu, S. Morgan, A. Allport, A. Cottrell, T. Do, J. McGregor, L. Wardhaugh, P. Feron, Results from trialling aqueous  $\text{NH}_3$  based post-combustion capture in a pilot plant at Munmorah power station: Absorption, *Chem. Eng. Res. Des.* 89 (2011) 1204–1215. doi:10.1016/j.cherd.2011.02.036.
- [2] F. Kozak, A. Petig, E. Morris, R. Rhudy, D. Thimsen, Chilled ammonia process for  $\text{CO}_2$  capture, *Energy Procedia*. 1 (2009) 1419–1426. doi:10.1016/j.egypro.2009.01.186.
- [3] D. Sutter, M. Gazzani, M. Mazzotti, A low-energy Chilled Ammonia Process exploiting controlled solid formation for post-combustion  $\text{CO}_2$  capture, *Faraday Discuss.* (2016). doi:10.1039/C6FD00044D.
- [4] K. Thomsen, P. Rasmussen, Modeling of vapor–liquid–solid equilibrium in gas–aqueous electrolyte systems, *Chem. Eng. Sci.* 54 (1999) 1787–1802. doi:10.1016/S0009-2509(99)00019-6.
- [5] V. Darde, W.J.M. van Well, E.H. Stenby, K. Thomsen, Modeling of carbon dioxide absorption by aqueous ammonia solutions using the Extended UNIQUAC model, *Ind. Eng. Chem. Res.* 49 (2010) 12663–12674.
- [6] D. Sutter, M. Gazzani, M. Mazzotti, Solid formation in ammonia-based  $\text{CO}_2$  capture processes - Thermodynamic analysis of criticalities and implications on process design, in: *Trondheim CCS Conf.*, 2015: p. June 18.
- [7] D. Sutter, M. Gazzani, M. Mazzotti, Formation of solids in ammonia-based  $\text{CO}_2$  capture processes—Identification of criticalities through thermodynamic analysis of the  $\text{CO}_2$ – $\text{NH}_3$ – $\text{H}_2\text{O}$  system, *Chem. Eng. Sci.* 133 (2015) 170–180. doi:10.1016/j.ces.2014.12.064.
- [8] J.-F. Pérez-Calvo, D. Sutter, M. Gazzani, M. Mazzotti, Application of a chilled ammonia-based process for  $\text{CO}_2$  capture to cement plants, *GHGT-13*, 2016 (submitted).
- [9] E.J. de Jong, A. Eble, C. Gahn, J. Garside, C. Heyer, M. Kind, A. Mersmann, J. Nyvlt, H. Offermann, J. Pohlisch, H. Schubert, *Measurement of crystal growth and nucleation rates*, 2nd ed., IChemE, Rugby, UK, 2002.
- [10] F. Franco, R. Anantharaman, O. Bolland, N. Booth, E. van Dorst, C. Edstrom, E. Sanchez Fernandes, E. Macchi, G. Manzolini, D. Nikolic, A. Pfeffer, M. Prins, S. Rezvani, L. Robinson, European best practice guidelines for assessment of  $\text{CO}_2$  capture technologies, CAESAR; Project no.: 213206, 2011.